Available online at www.sciencedirect.com
SCIENCE DIRECT®

Journal of the European Ceramic Society 24 (2004) 2567–2574
www.elsevier.com/locate/jeurceramsoc

Impedance spectroscopy of $Bi_4Ti_3O_{12}$ ceramic produced by self-propagating high-temperature synthesis technique

Z.S. Macedo[a], C.R. Ferrari[b], A.C. Hernandes[b,*]

[a]*Universidade Federal de Sergipe, Departamento de Física. Cx Postal: 353, 49100-000 São Cristovão, SE, Brazil*
[b]*Universidade de São Paulo, Instituto de Física de São Carlos, Grupo Crescimento de Cristais e Materiais Cerâmicos, Cx Postal: 369, 13560-970 São Carlos, SP, Brazil*

Received 8 January 2003; received in revised form 5 August 2003; accepted 27 September 2003

Abstract

$Bi_4Ti_3O_{12}$ (bismuth titanate—BIT) ferroelectric ceramic was synthesized by self-propagating high-temperature synthesis (SHS) technique. The microstructure, electric and dielectric properties were determined and the results were compared to a reference sample produced by solid state reaction. The powders from SHS had agglomerated particles with average size of 200 nm. $Bi_4Ti_3O_{12}$ 100% crystalline phase was reached after SHS reaction followed by sintering at 1050 °C/2 h. The sintered bodies presented high relative density (98%) and small grain size (around 5 microns). The electrical and dielectric properties of the samples were studied using the impedance spectroscopy technique, and the three observed semicircles in the complex impedance diagrams were associated to the bulk, plate boundaries and grain boundaries of the sintered ceramics. The samples produced through SHS presented the same bulk conductivity as the reference one, and lower conductivity of the grain and plate boundaries. The same dielectric constant $\varepsilon' = 200$, at 300 °C and $f = 1$ MHz, was found for SHS sample and for the reference. For higher temperatures, at this same frequency, SHS samples presented higher relative permittivity than the reference, and for temperatures above T_c both samples presented the same Curie–Weiss parameters. The differences observed in the electrical conductivity and relative permittivity, were attributed to the differences in the grain size and defect concentration. The anomaly in the permittivity curves near 550 °C is also discussed.

Keywords: $Bi_4Ti_3O_{12}$; Dielectric properties; Electrical properties; Impedance spectroscopy; SHS

1. Introduction

Bismuth titanate ($Bi_4Ti_3O_{12}$, or BIT) is a bismuth layer structured ferroelectric discovered by B. Aurivillius in 1949.[1] Its crystalline structure consists of $(Bi_2Ti_3O_{10})^{-2}$ layers formed by $BiTiO_3$ unit cells of perovskite-like structures alternating with $(Bi_2O_2)^{2+}$ layers perpendicular to the *c* axis.[1,2] This plate-like morphology gives rise to electrical anisotropy with the higher component of its spontaneous polarisation ($P_5 \sim 50$ μC/cm^2) parallel to the bismuth layers.[3–5] $Bi_4Ti_3O_{12}$ high Curie temperature (670 °C) gives it wide applicability in electronic elements, as transducers, piezoelectric and memory devices.[6,7] Due to its importance in the electronic industry, a great deal of synthesis routes had been proposed to obtain BIT single crystals, ceramics and thin films with suitable properties.[8–10] There are some few papers reporting BIT production by self-propagation high-temperature synthesis (SHS)[11,12] and to our knowledge the electrical and dielectric properties of this product have not been reported yet.

SHS, also known as combustion synthesis, is an attractive technique to produce ceramic materials since it is a simple and efficient process. The technique consists on heating a homogeneous mixture of metal salts, oxides and/or carbonates and a suitable organic fuel. The high temperature is induced by a self-sustained exothermic chemical reaction, whose ignition temperature is lower than the crystallisation temperature of the product.

There is a substantial economic benefit in the SHS production, and for this reason, it has been widely used

* Corresponding author. Tel.: +55-16-273-9828; fax: +55-16-273-9824.
E-mail address: hernandes@if.sc.usp.br (A.C. Hernandes).

0955-2219/$ - see front matter © 2003 Elsevier Ltd. All rights reserved.
doi:10.1016/j.jeurceramsoc.2003.09.026

in the synthesis of various compounds.[13–15] According to Merzhanov,[16] SHS products and conventionally produced ceramics (solid state route) have a ratio of cost that ranges from 0.4 to 0.13. The goal of many researchers working on combustion synthesis of advanced materials is to produce these materials with comparable or possibly superior properties to those produced by other ceramic processing techniques.

In a previous paper,[11] we have related a series of SHS experiments to produce BIT, exploring different fuels and experimental conditions, as annealing temperatures and stoichiometric ratios. The aim of the present work is to discuss the characterisation of BIT ceramics produced by SHS, comparing their microstructure, electrical and dielectric properties to those observed for samples produced by conventional solid-state reaction.

2. Experimental

$Bi_4Ti_3O_{12}$ produced through combustion synthesis route will be called BIT–SHS hereafter. The starting materials were TiO_2 (Vetec, 99.8%) and $Bi(NO_3)_3.5H_2O$ (Mallinckrodt, 99.98%), in excess of 3%-w, used as cation precursors, and $CO(NH_2)_2$ (urea) (Merck, 99.5%) used as fuel. The reactants were firstly mixed to about 5 ml of distilled water and homogenised in a quartz crucible. The synthesis was carried out by heating the mixture in air using an electric plate at 450 °C. At this temperature the ignition took place. The reaction lasted less than 5 min and produced a dry, yellowish to brownish powder. In some cases the BIT–SHS powder was annealed at 1000 °C/30 min before the sintering step.

BIT was also prepared by solid-state reaction to be used as reference. In this case, the precursor powders Bi_2O_3 and TiO_2 (Alfa Aesar, 99.99%) were mixed in the stoichiometric proportion and ball-milled for 3 h in plastic recipients containing the powders, zirconia balls and isopropyl alcohol in the volumetric proportion of 10:60:30. The as-dried material was calcined at 750 °C for 3 h in Pt crucible in an open atmosphere furnace. The calcined powders were milled again for 108 h and calcined at 750 °C for 10 h.

The ceramic powders obtained from both methods were pelletized and sintered following the same procedure. The powders were mixed with a binder solution of polyvinyl alcohol in an agate mortar, pressed uniaxially (~20 MPa) and sintered at 1050 °C for 2 h.

The thermal analysis of the produced powders was performed in DTA equipment (TA Instruments 1600 DTA) and the crystalline phase obtained was identified by X-ray diffraction (XRD) (Rigaku Rotaflex–RU-200B) in continuous scanning mode. A Zeiss DSM960 Scanning Electron Microscope (SEM) was used to investigate particle size and morphology. The density of the sintered specimens was determined by the method of fluid displacement (Archimedes method) using distilled water.

For the impedance spectroscopy measurements, the ceramic disks were polished with alumina powder, cleaned with acetone in ultrasonic bath for 15 min and dried at 100 °C. Electric contact was made by applying Pt paste on the parallel faces of the pellet and firing it at 700 °C for 30 min. The measurements were performed in the frequency range from 5 Hz to 13 MHz, with an applied potential of 500 mV, using a Solartron 1260 Impedance Analyzer controlled by a personal computer. These ac measurements were taken isothermally, at temperatures from 300 up to 750 °C, and the results were analysed using the software Zview.[17]

3. Results and discussions

3.1. Powder characteristics

Fig. 1 shows the XRD patterns of BIT–SHS as produced (curve a), after annealing at 1000 °C/0.5 h (curve b) and after sintering at 1050 °C/2 h (curve c). The peaks identified at curve 1(a) were associated to the phases TiO_2, $Bi_{12}TiO_{20}$ and $Bi_2Ti_2O_7$. After annealing for 30 min, $Bi_4Ti_3O_{12}$ was the predominant phase but a very little amount of the phases $Bi_2Ti_2O_7$ and $Bi_{12}TiO_{20}$ were still found, possibly because longer times would be necessary to complete the formation of the crystalline $Bi_4Ti_3O_{12}$. In fact, the pellets sintered for 2 h exhibited the unique phase $Bi_4Ti_3O_{12}$, as shown in Fig. 1—curve c. The XRD pattern of the reference sample, produced

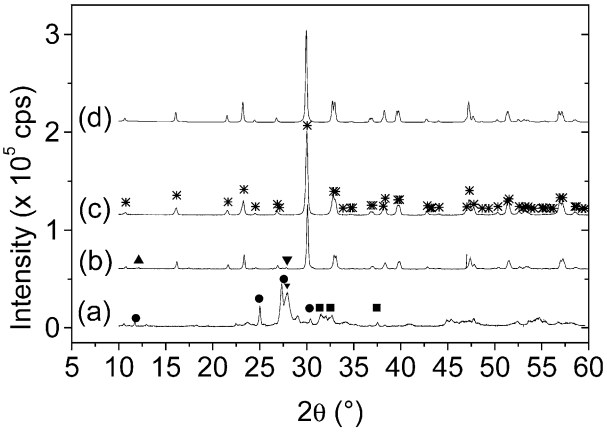

Fig. 1. Powder XRD patterns of the samples produced by SHS (curves a, b and c): (a) before annealing, (b) after annealing at 1000 °C/30 min, (c) after conforming and sintering at 1050 °C/2h. Curve (d): reference sample, produced by solid state reaction. Indexed crystalline phases from JCPDS collection: *—$Bi_4Ti_3O_{12}$ (file number 73-2181), ▲ $Bi_2Ti_4O_{11}$ (file number 32-0118), ▼—$Bi_{12}TiO_{20}$ (file number 42-0186), •—$Bi_2Ti_2O_7$ (file number 72-1820), ■. TiO_2 (file number 84-1750).

by solid state reaction, also presented the single phase $Bi_4Ti_3O_{12}$ (Fig. 1—curve d).

BIT–SHS presented mean particle size of 200 nm (see Fig. 2a), and for the reference sample this value was 1 μm (Fig. 2b). A great number of agglomerates can be seen in the BIT–SHS powder, which is typical of combustion synthesis products. The milling in agate mortar before compacting and sintering was adopted in order to break the agglomerates. It was also observed that the annealing step before conformation induces some undesirable coalescence of the inter-agglomerate particles. These agglomerates were more difficult to break in the mortar, leading to a decrease in the final density of the sintered ceramic, as will be discussed in the next section.

3.2. Density and microstructure

The relative density of the BIT sintered ceramics was determined for the samples prepared according to three different procedures: (1) the powder from SHS was annealed at 1000 °C for 30 min, then conformed and sintered at 1050 °C/2 h; (2) the powder from SHS was simply conformed and sintered at 1050 °C/2 h and (3) BIT was synthesised by solid-state reaction, sintered under the same experimental conditions and used as reference. The second and third cases provided ceramics with high relative density, both near 98%. The annealing step of the SHS powder before conformation was tested since it had been previously determined as an essential step to produce BIT,[11,12] but samples annealed before conformation achieved final density of only 90%. The presence of agglomerates is a general feature of powders produced by combustion synthesis, and this is the main cause of the porosity observed in those sintered ceramics since the intra-agglomerate particles undergo the sintering process at a lower temperature than the inter-agglomerate ones. As the sintering without annealing also yielded single phase $Bi_4Ti_3O_{12}$, it was adopted in the production of the samples for further characterisation.

The sintered ceramics presented grains with plate-like morphology and average grain size about 5 μm for BIT–SHS (Fig. 3a) and about 14 μm for the reference samples (Fig. 3b), measured along the larger dimension of the platelets. The aspect ratio (length/thickness) of the sintered grains seemed to be the same for both samples.

3.3. Electrical properties

Impedance diagrams of BIT–SHS and reference sample are presented in Fig. 4. Three semicircles are well resolved, each of them corresponding to the impedance of a different microstructural region of the ceramic. The electrical resistivity of each region is characterised by the diameter of the corresponding normalised semicircle and the maximum of each semicircular arc corresponds to the relaxation frequency. The three arcs observed were enumerated as 1st, 2nd and 3rd from the left to the right in the graphs, in crescent order of frequency. Electrode polarisation caused only a slight enhancement of the noise levels for measurements at frequencies lower than 100 Hz, so it was not taken into account for the data fitting.

The ac properties of BIT single crystals were reported by Huanosta et al.[18] and Kim et al.[19] and the complex diagram of BIT single crystal was characterised by the presence of two semicircles, in measurements perpendicular to the ab plane. Huanosta et al.[18] observed that each BIT single crystal presented a mica-like aspect

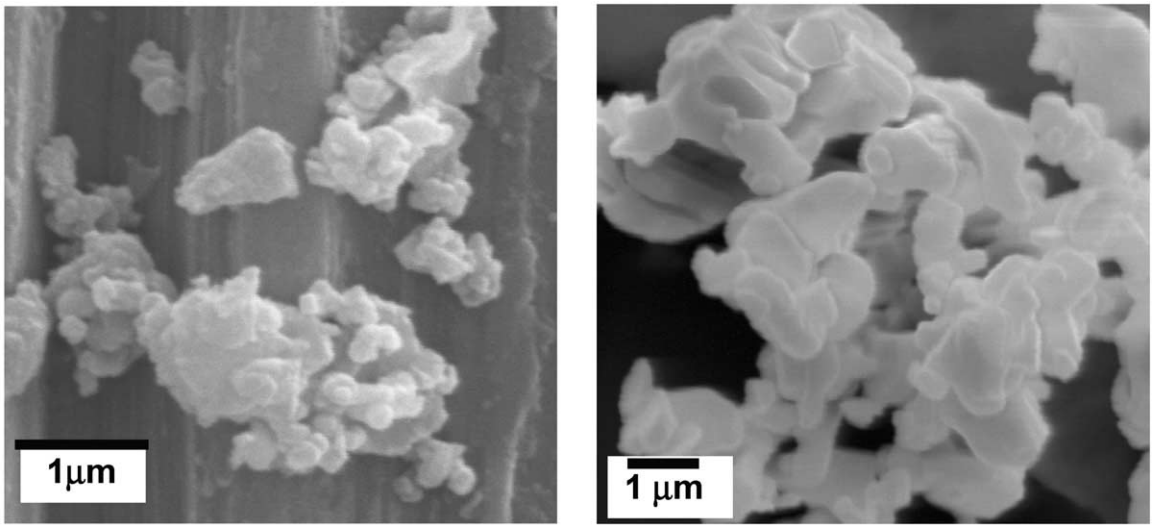

Fig. 2. SEM micrographs of $Bi_4Ti_3O_{12}$ powders: (a) produced by SHS; (b) produced by solid-state reaction.

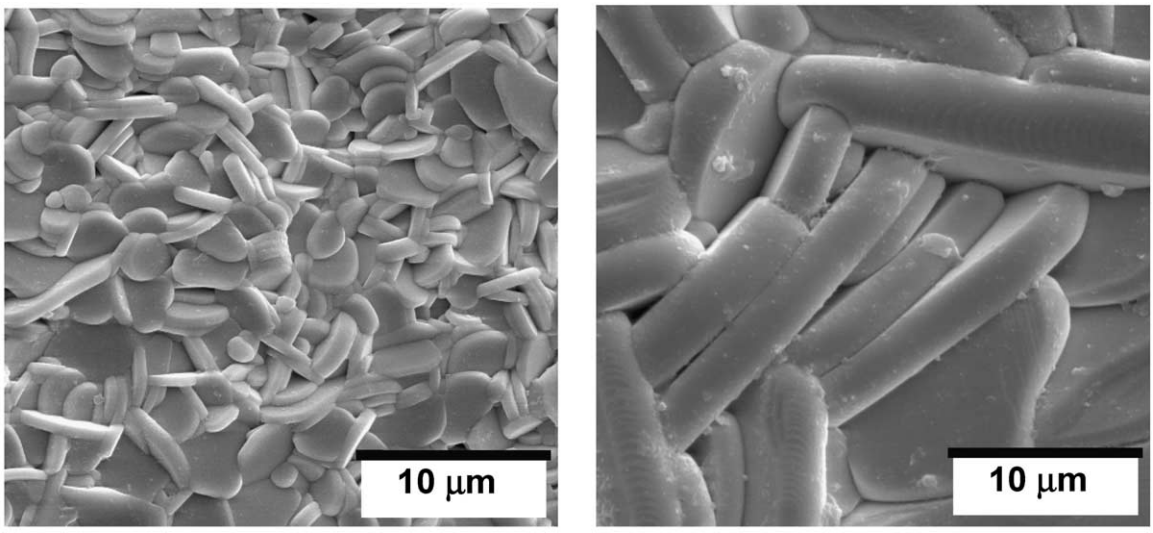

Fig. 3. SEM photographs of $Bi_4Ti_3O_{12}$ compacts sintered at 1050 °C for 2 h: (a) produced by SHS; (b) produced by solid-state reaction.

consisted of piled up crystalline plates. Based on this observation, they interpreted the two impedance semicircles of the single crystal as the separated contributions from the crystalline plates and the plate boundary regions.

Accordingly, each grain in the polycrystalline sample is formed by piled up crystalline plates, so the three semicircular arcs observed in Fig. 4 can be attributed to the contributions from the grain boundaries (1st arc), plate boundaries (2nd arc) and bulk of the crystalline plates (3rd arc). The arcs in Fig. 4 were depressed, indicating a deviation from the Debye behaviour.[20,21]

The brick-layer model[20] was employed to represent the electrical response of BIT ceramics. In this material, the impedances of three different microstructural regions were present in the ceramic, so the electrical properties were determined by a series combination of such impedances. The equivalent electric circuit proposed is presented in Fig. 5. Each arc from the experimental data was represented by a parallel combination of a resistance (R) and a constant-phase element (CPE).

The CPE is an empirical impedance function with considerable importance in data fitting. It substitutes the uniquely capacitive element, in order to account for the depression of the semicircles when the sample presents a non-Debye behaviour.[20] When the capacitance is substituted by a CPE element, the impedance is expressed by the phenomenological equation.[21]

$$Z = \frac{R}{1 + (i\omega RC)^{\Psi}} \tag{1}$$

where $0 \leqslant \Psi \leqslant 1$ and $i = \sqrt{-1}$. The parameter Ψ depends on the distribution width of the relaxation times around a mean value $\tau_0 = RC$. When $\Psi = 1$, Eq. (1) reduces to the impedance of a simple RC element.

The theoretical curves as well as the deconvoluted arcs were plotted in Fig. 4. As it can be observed, the experimental response was in excellent agreement with the theoretical one thus indicating that the proposed model gave an adequate representation of the electrical properties of the samples. It was not necessary to include an impedance element representing the ceramic–electrode interface in this case since the contact impedance was small.

Three R values were obtained from each fitting. They represented the normalised electrical resistances of the three different microstructural regions in the ceramic at a specific temperature. Considering the characteristic anisotropy of BIT conductivity and the random orientation of the grains, our results correspond to intermediate values between the components parallel and perpendicular to the c axis.

The electrical conductivity values were calculated from the resistance values. Fig. 6 shows the log plots of the electric conductivity as a function of the reciprocal temperature, for temperatures between 300 and 750 °C. For BIT–SHS samples, higher conductivities for the crystalline plates and grain boundaries were observed, while the plate boundaries presented lower conductivity than the reference. The enhancement observed for the conductivities can be attributed to higher concentration of defects in BIT–SHS samples, since smaller conductivities were expected for the BIT ceramic that possesses smaller sintered grains.[4]

The conductivities from the three separate contributions followed the Arrhenius law

$$\sigma(t) = \sigma_0 \exp(-E_a/kT), \tag{2}$$

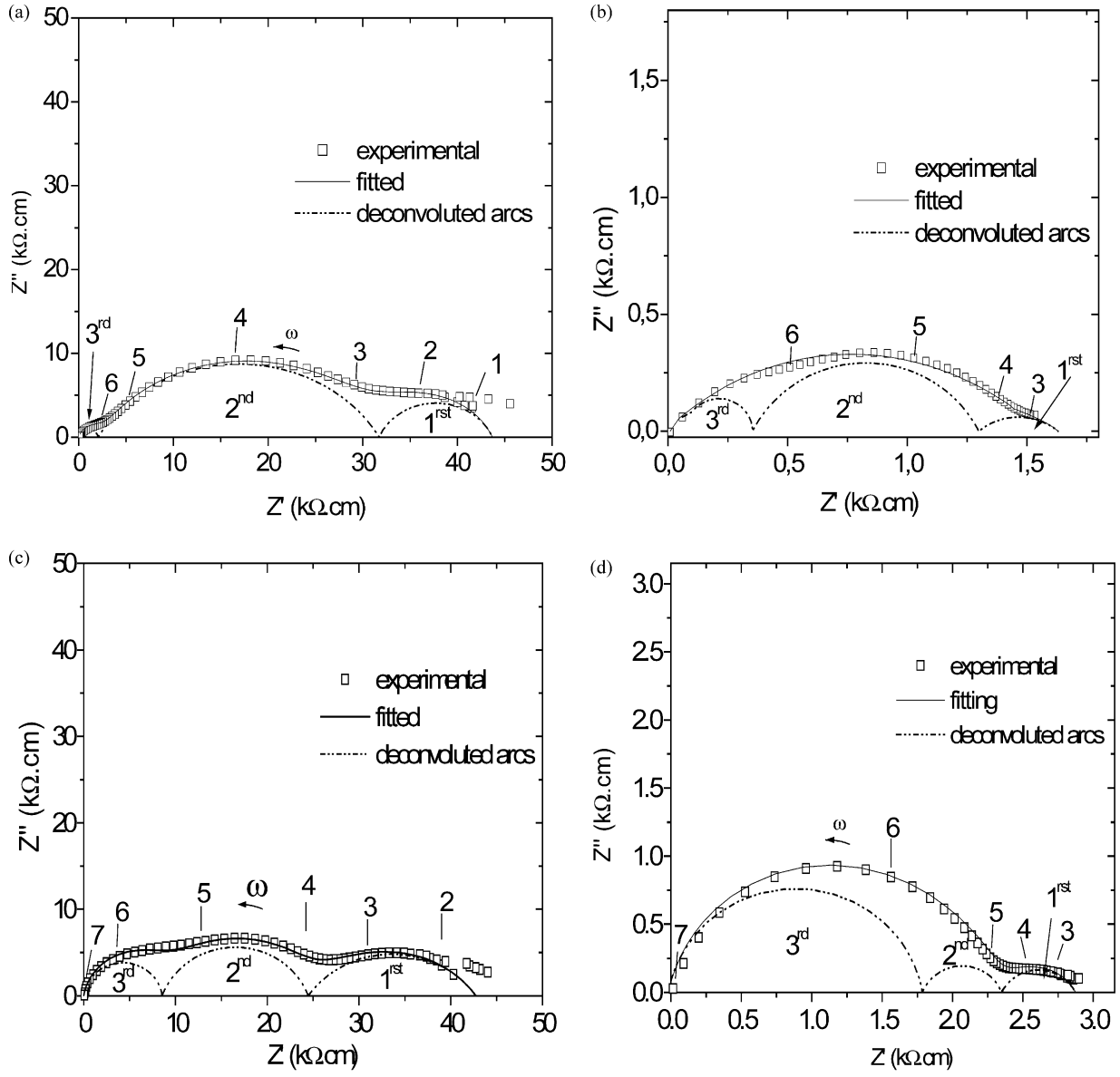

Fig. 4. Impedance diagrams of sintered ceramics (1050 °C/2 h): (a) BIT–SHS measured at 500 °C; (b) BIT–SHS measured at 710 °C; (c) reference sample measured at 500 °C and (d) reference sample measured at 710 °C. The numbers indicate the logarithm of signal frequency. The arcs were enumerated as 1st, 2nd and 3rd, in crescent order of frequency.

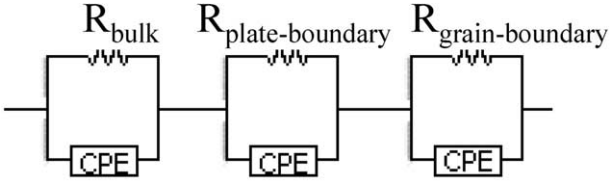

Fig. 5. Equivalent circuit used to represent the impedance response of BIT ceramics.

where σ_0 is a pre-exponential factor and E_a, k and T represent the apparent activation energy for the conduction process, Boltzmann' constant and the absolute temperature, respectively. The apparent activation energies, indicated in Fig. 6, were deduced from the slope of the straight-line regions. Below T_c, the activation energies calculated for BIT–SHS agree with the values determined for the reference sample. Furthermore, the activation energy determined for the crystalline plates agree with that reported by Huanosta et al.,[18] and the energy values determined for both plate boundaries and grain boundaries were found to be the same. These results indicate the same conduction process and similar energy barriers for grain boundaries and plate boundaries.

The random orientation of the grains did not allow us to separate the contribution from the two directions of the plate-like grains, so the measured conductivity of the crystalline plates is expected to reflect an inter-

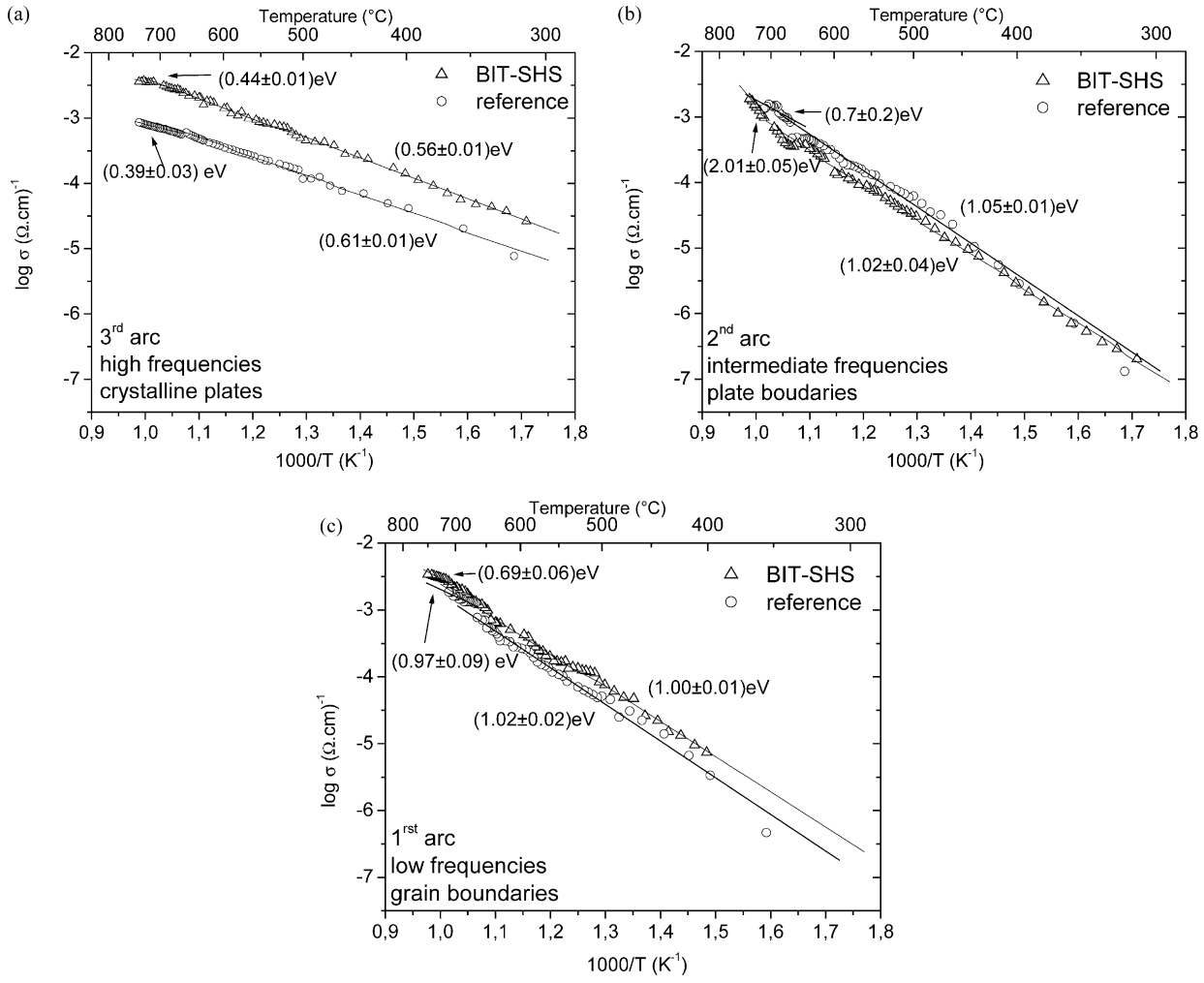

Fig. 6. Ahrrenius plot of BIT produced by solid-state reaction and BIT produced by SHS synthesis. The electric conductivities were determined from the arcs in the impedance diagram. (a) high frequency arc; (b) intermediate arc; (c) low-frequency arc.

mediate value between the carriers mobility along the *c* axis and *a* (or *b*) axis.

The changes observed in the apparent E_a near $T_c = 670$ °C were related to changes in the predominant conduction mechanism. Kim et al.[19] reported BIT conduction as *n*-type below T_c and *p*-type above T_c, but Shulman et al.[22] suggested the opposite behaviour, with p-type conduction below T_c and *n*-type conduction above T_c. On the other hand, the $(Bi_2O_2)^{2+}$ layers are known as ionic conductors in some materials belonging to the Aurivillius family,[5] and oxygen vacancies in the perovskite layers would also lead to ionic conduction in this region. The hypothesis of electronic conduction combined to localised ionic movement is also very acceptable, as will be seen in the next section.

3.4. Dielectric properties

The complex permittivity ε;* was obtained from the complex impedance data Z^* by the expression.[20]

$$\varepsilon^* = \left(i\omega\varepsilon_0 \frac{S}{\ell} Z^* \right)^{-1} = \varepsilon' + i\varepsilon'' \tag{3}$$

where S is the electrode area, ℓ is the pellet thickness and ε;$_0$ is the vacuum permittivity. The real component ε;′ is the relative permittivity, or dielectric constant, and the imaginary part ε;″ is the loss factor.

Fig. 7 a shows the relative permittivity of BIT–SHS and reference sample, as a function of the temperature, at several frequencies. It can be seen that the relative permittivity undergoes a low-frequency dispersion for all temperatures measured, due to the presence of conduction mechanisms in the material. In this case, charge carriers have to be considered in the polarisation mechanisms,[23,24] and the relative permittivity presents a conductive component (Iσ/ω). The dipolar behaviour of both BIT–SHS and reference sample is more evident for frequencies higher than 10^4 Hz. Above this frequency the permittivity curves presented a well-defined peak at T_c.

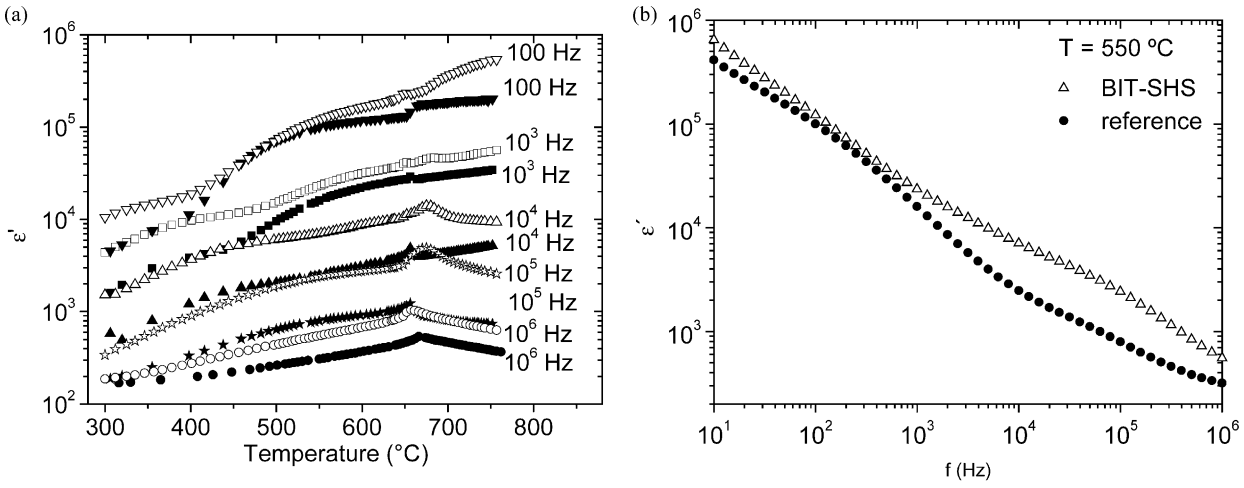

Fig. 7. Relative permittivity of BIT–SHS and reference sample: (a) ϵ' as a function of the temperature, for frequencies between 1 kHz and 1 MHz. Open symbols: BIT–SHS; solid symbols: reference sample; (b) ϵ' as a function of the frequency, at $T = 550$ °C.

The anomalous peak near 550 °C, observed in Fig. 7a, was reported previously by several researchers[19,25–27] and was attributed to phenomena such as structural changes,[19] space-charge relaxation[25] and oxygen vacancy movement.[26,27] Shulman et al.[27] have shown that niobium doped samples had the relaxation at 550 °C suppressed, and have suggested that Nb ions would prevent from oxygen vacancy formation. These authors proposed a polarisation mechanism due to local ionic jumps to explain the anomalous behaviour of BIT near 550 °C.

In fact, the peak at 550 °C was less pronounced at $f = 10^6$ Hz (see Fig. 7a), which reinforces the idea of a slow phenomenon, such as ionic polarisation or space charge relaxation, occurring predominantly at the grain boundaries and plate boundaries. In single crystals, where the anomaly was also observed,[19] the phenomenon would occur mainly in the plate boundaries.

Fig. 7b illustrates the permittivity versus frequency for BIT–SHS and for the reference ceramic, at 550 °C. The frequency interval from 10 Hz to 10^3 Hz corresponds approximately to the grain boundary response. In this frequency interval the relative permittivity was dominated by the conductive term, so the higher BIT–SHS permittivity can be due to the slight enhancement in the conductivity (see Fig. 6c) of the grain boundaries. The greatest differences in $\varepsilon;'$ were observed in the frequency interval from 2.10^3 to 5.10^5 Hz, corresponding approximately to the relaxation frequencies of the intermediate semicircle of Fig. 4. Since the conductivity of the plate boundaries did not increase in BIT–SHS (see Fig. 6b), the enhancement of $\varepsilon;'$ at these frequencies should be due to a localised charge movement at this microstructural region. For frequencies near 10^6 Hz, which correspond to the contribution from the crystalline plates, the conductive term ($i\sigma/\omega$) is small since the frequency is high, so the enhancement in the permittivity should be due to the smaller grain size.[4]

From the above results, we conclude that at least three simultaneous mechanisms can be present at BIT ceramics under an alternating external field: (1) electronic conduction, as reported in references 19 and 22; (2) re-orientation of the spontaneous dipoles, typical of ferroelectric materials, and (3) polarisation at the plate boundaries, which is probably due to localised ionic jumps as suggested in reference 27 and do not contribute to the electronic conductivity. The electronic conduction and ionic local polarisation could be both due to oxygen vacancies in different microstructural regions of the sample, but more evidence is necessary to define the defects related to each mechanism.

In order to attest the quality of BIT–SHS samples, we have compared the relative permittivity values at $f = 1$ MHz (Fig. 8). For $T = 300$ °C, one can observe that both samples presented the same value $\varepsilon;' = 200$, which agreed with the values reported in the literature.[3,27,28] Above 400 °C the difference between the relative permittivity of BIT–SHS and the reference sample increased, up to the ferro/paraelectric transition temperature (T_c). At $f = 1$ MHz and $T = T_c$, both curves reached a maximum, with $(\varepsilon;'_{max})_{BIT-SHS} = 1040$ and $(\varepsilon'_{max})_{reference} = 530$.

The permittivity data at 1 MHz were fitted to the Curie–Weiss function

$$\varepsilon' = C/(T - T_0) \quad (4)$$

for temperatures higher than T_c. The obtained Curie–Weiss temperatures (T_0) were 506 and 455 °C and the Curie constants (C) were $1.58.10^5$ °C and $1.09.10^5$ °C for BIT–SHS and reference sample, respectively. These values are in good agreement with the parameters determined by Fouskova et al.[21] for BIT single crystal,

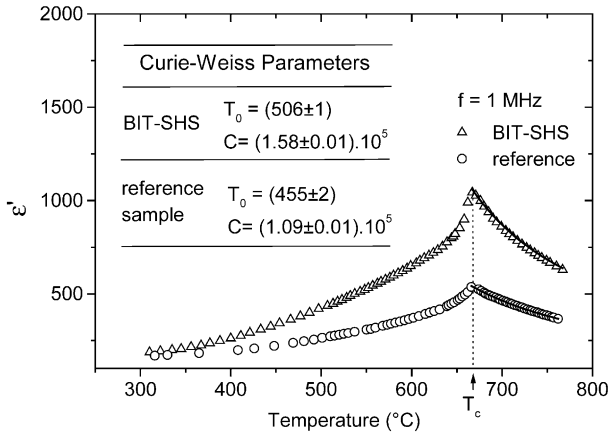

Fig. 8. Relative permittivity of BIT produced by solid-state reaction and BIT–SHS, fitted by the Curie–Weiss law for temperatures above T_c.

measured at 5 MHz. The similarity of the fitted parameters C and T_0 for the both samples studied again attests the efficiency of the SHS technique to obtain BIT with reasonable good properties.

4. Conclusions

Our main goal in this paper was to show that BIT produced by SHS presented electrical and dielectric properties comparable to that observed for the conventional samples.

The sintered ceramics obtained through SHS reached high density (98% theoretical) and 100% single phase, in approximately 5 min of reaction and 2 h of sintering, whereas the conventional process took more than 100 h. The reduced processing time, the simplicity of the procedure and the excellent quality of the produced material are the greatest advantages of SHS method.

Three relaxation processes were observed, corresponding to three different microstructural regions in the BIT ceramic (crystalline plates, plate boundaries and grain boundaries). The good physical properties of BIT–SHS sintered ceramics attest their applicability in the same electrical devices, which employ the conventionally produced ceramics. BIT–SHS presented similar activation energies for the conduction processes, the same dielectric permittivity at 300 °C, the same Curie temperature ($T_c = 670$ °C) and Curie-Weiss parameters. Some differences observed in the overall conductivity, and also in the real permittivity (at high frequencies and temperatures above 300 °C), can be related to the smaller grains of BIT–SHS and to the density of defects in the samples. The main features observed for the relative permittivity were: (1) the low frequency dispersion is due to the conductive term; (2) the anomalous peak is related to polarisation in the boundaries; (3) the difference between BIT–SHS and the reference sample is higher between 2.10^3 Hz and 5.10^5 Hz, probably due to ionic polarisation at the plate boundaries.

Acknowledgements

The authors gratefully acknowledge FAPESP, CAPES and CNPq by the financial support.

References

1. Aurivillius, B., *Arkiv for Kemi*, 1949, **1**, 499.
2. Jovalekic, C. and Stevic, S., *Ferroelectrics*, 1992, **132**, 185.
3. Cummings, S. E. and Cross, L. E., *J. Appl. Phys.*, 1968, **39**, 2268.
4. Villegas, M., Caballero, A. C., Moure, C., Durán, P. and Fernández, J. F., *J. Am. Ceram. Soc.*, 1999, **82**, 2411.
5. Irie, H., Miyayama, M. and Kudo, T., *J. Am. Ceram. Soc.*, 2000, **83**, 2699.
6. Pintilie, L., Alexe, M., Pignolet, A. and Hesse, D., *Appl. Phys. Lett.*, 1998, **73**, 342.
7. Dawley, J. T., Radspinner, R., Zelinski, B. J. J. and Uhlmann, D. R., *J. Sol-Gel Sd. Techn.*, 2001, **20**, 85.
8. Takahashi, J., Kawano, S., Shimada, S. and Kageyama, K., *Jpn. J. Appl. Phys*, 1999, **38**, 5493.
9. Araüjo, E. B. and Eiras, J. A., *J. Phys. D: Appl. Phys.*, 1999, **32**, 957.
10. Takeuchi, T., Tani, T. and Saito, Y., *Jpn J. Appl. Phys*, 1999, **38**, 5553.
11. Macedo, Z. S., Ferrari, C. R. and Hernandes, A. C., Self Propagation High Temperature Synthesis of $Bi_4Ti_3O_{12}$, *Powder Technology* (2003).
12. Sych, A. M., Nedil'ko, L. F. and Kuz'min, R. N., *Inorganic Materials*, 1999, **35**, 290.
13. Lee, J. W., Munir, Z. A., Shibuya, M. and Ohyanagi, M., *Journal of the American Ceramic Society*, 2001, **84**, 1209.
14. Poth, J., Haberkom, R. and Beck, H. P., *Journal of European Ceramic Society*, 2000, **20**(6), 715–723.
15. Fumo, D. A., Morelli, M. R. and Segadaes, A. M., *Materials Research Bulletin*, 1996, **31**, 1243.
16. Merzhanov, A. G., *Ceramics International*, 1995, **21**, 371.
17. Jonhson, D. Software Zview—v.2.3d, Scribner Associates, Inc. (2000).
18. Huanosta, A., Alvarez-Fregoso, O. and Amano, E., *J. Appl. Phys.*, 1991, **69**, 404.
19. Kim, S. K., Miyayama, M. and Yanagida, H., *Materials Research Bulletin*, 1996, **31**(1), 121.
20. Macdonald, J. R., *Impedance Spectroscopy—Emphasizing Solid Materials and Systems*. John Wiley & Sons, 1987.
21. Cole, K. S. and Cole, R. H., *J. Chem. Phys.*, 1941, **9**, 341.
22. Shulman, H. S., Testorf, M., Damjjanovid, D. and Setter, N., *J. Am. Ceram. Soc.*, 1996, **79**(12), 3124–3128.
23. Elissalde, C. and Ravez, J., *Journal of Materials Chemistry*, 2001, **11**(8), 1957–1967.
24. Jonscher, A. K., *Philosophical Magazine B*, 1978, **38**(6), 587–601.
25. Fouskova, A. and Cross, L. E., *J. Appl. Phys.*, 1970, **41**, 2834.
26. Jiménez, B., Jiménez, R., Castro, A., Millán, P. and Pardo, L., *J. Phys.: Condens. Matter*, 2001, **13**, 7315–7326.
27. Shulman, H. S., Damjjanovid, D. and Setter, N., *J. Am. Ceram. Soc.*, 2000, **83**(3), 528–532.
28. Villegas, M., Moure, C., Fernandez, J. F. and Duran, P., *Ceramics International*, 1996, **22**, 15.